Supplementary information

Characterization of offline analysis of particulate matter with FIGAERO-CIMS

Jing Cai[1,2,#], Kaspar R. Daellenbach[1,2,3,#,*], Cheng Wu[4,5], Yan Zheng[6], Feixue Zheng[1], Wei Du[1,2], Sophie L. Haslett[4], Qi Chen[6], Markku Kulmala[1,2], Claudia Mohr[4,*]

[1] Aerosol and Haze Laboratory, Beijing Advanced Innovation Center for Soft Matter Science and Engineering, Beijing University of Chemical Technology, Beijing 100029, China

[2] Institute for Atmospheric and Earth System Research, Faculty of Science, University of Helsinki, Helsinki 00014, Finland

[3] Laboratory of Atmospheric Chemistry, Paul Scherrer Institute, Villigen, Switzerland.

[4] Department of Environmental Science, Stockholm University, Stockholm, 11418, Sweden

[5] Department of Chemistry and Molecular Biology, Atmospheric Science, University of Gothenburg, Gothenburg, SE-412 96, Sweden

[6] State Key Joint Laboratory of Environmental Simulation and Pollution Control, Beijing Innovation Center for Engineering Science and Advanced Technology, College of Environmental Science and Engineering, Peking University, Beijing, 100871, China

[#] These authors contributed equally to this work.

Correspondence to: kaspar.daellenbach@helsinki.fi and claudia.mohr@aces.su.se

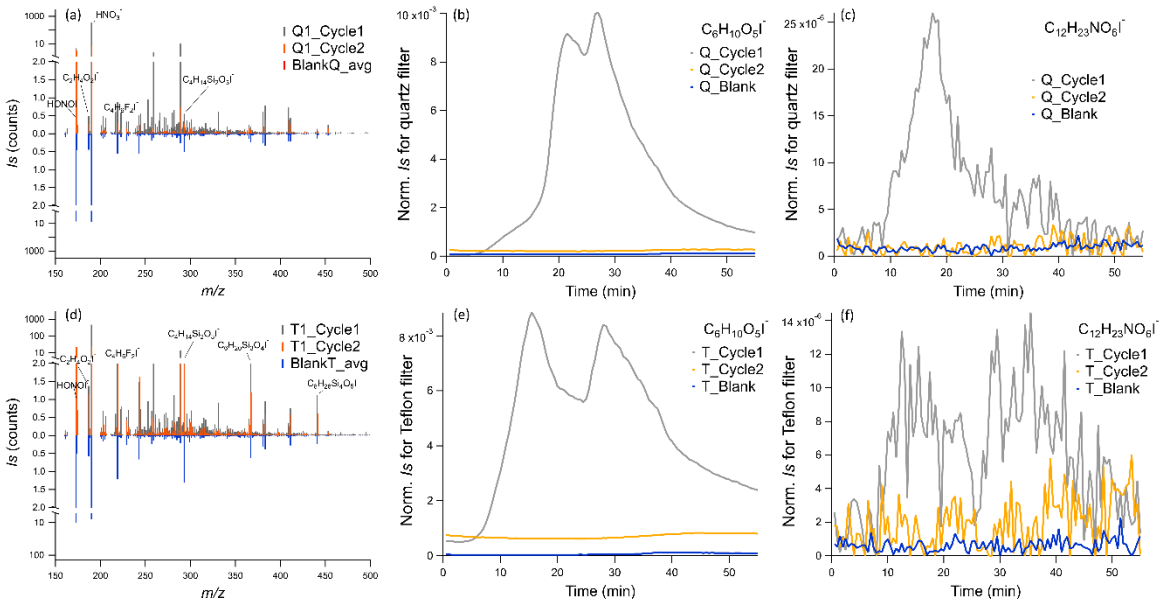

Figure S1. Comparison of the integrated raw signals from heating, reheating cycles and ambient blanks for (a) Quartz fiber filters and (d) Teflon filters, thermograms of $C_6H_{10}O_5I^-$ (b) and $C_{12}H_{23}NO_6I^-$ (c) of heating and reheating cycles for Quartz fiber filters, and thermograms of $C_6H_{10}O_5I^-$ (e) and $C_{12}H_{23}NO_6I^-$ (f) of heating and reheating cycles for Teflon filters.

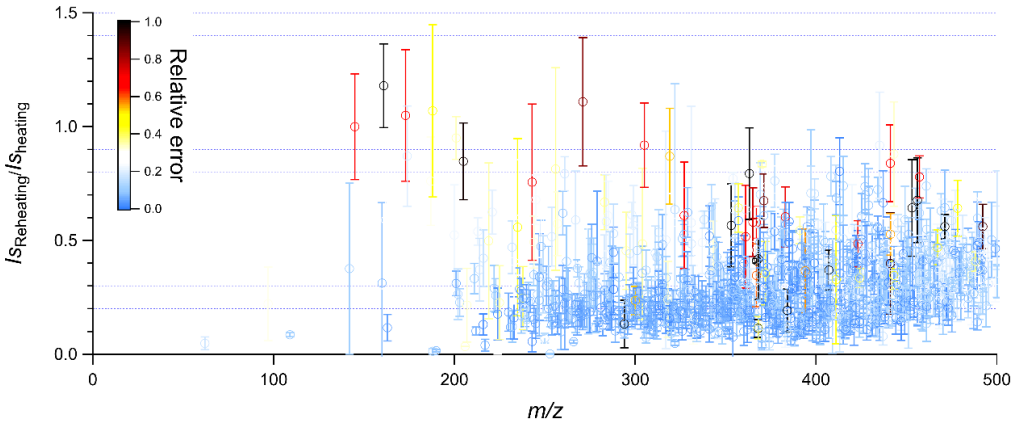

Figure S2. The average *Is* ratios between reheating and heating cycles for the Quartz filter with the standard deviations for the three reheating tests. Dots were colored by the relative errors (defined as the Std/Avg of *Is* from the duplicate tests) of compounds

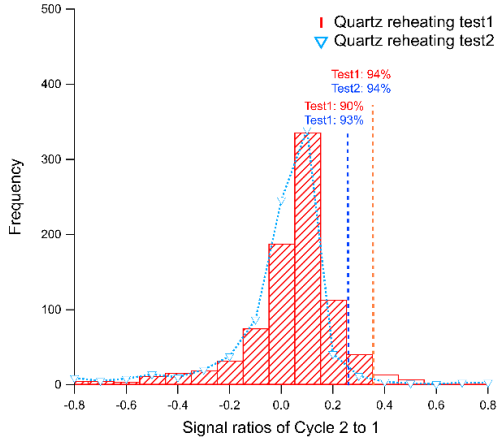

Figure S3. The distribution of *Is* ratios from reheating/heating for 0.75 and 1.2 μg loading Quartz samples. The negative value is caused by the low signals of the reheating cycles and background subtractions.

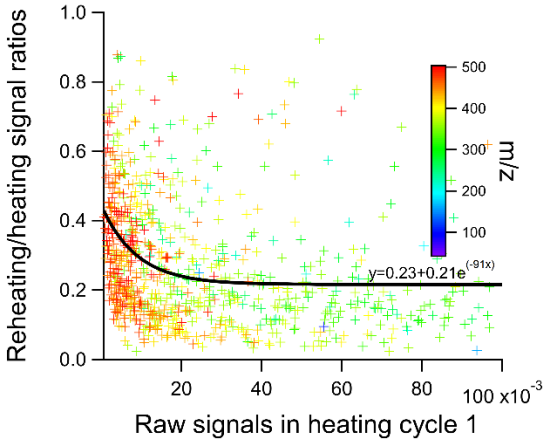

Figure S4. Exponential fit for reheating/heating signal ratios

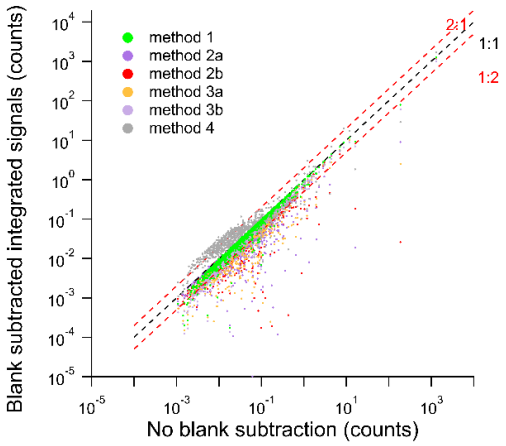

Figure S5. Comparison of the integrated signals for the 24-h samples for different blank subtraction methods

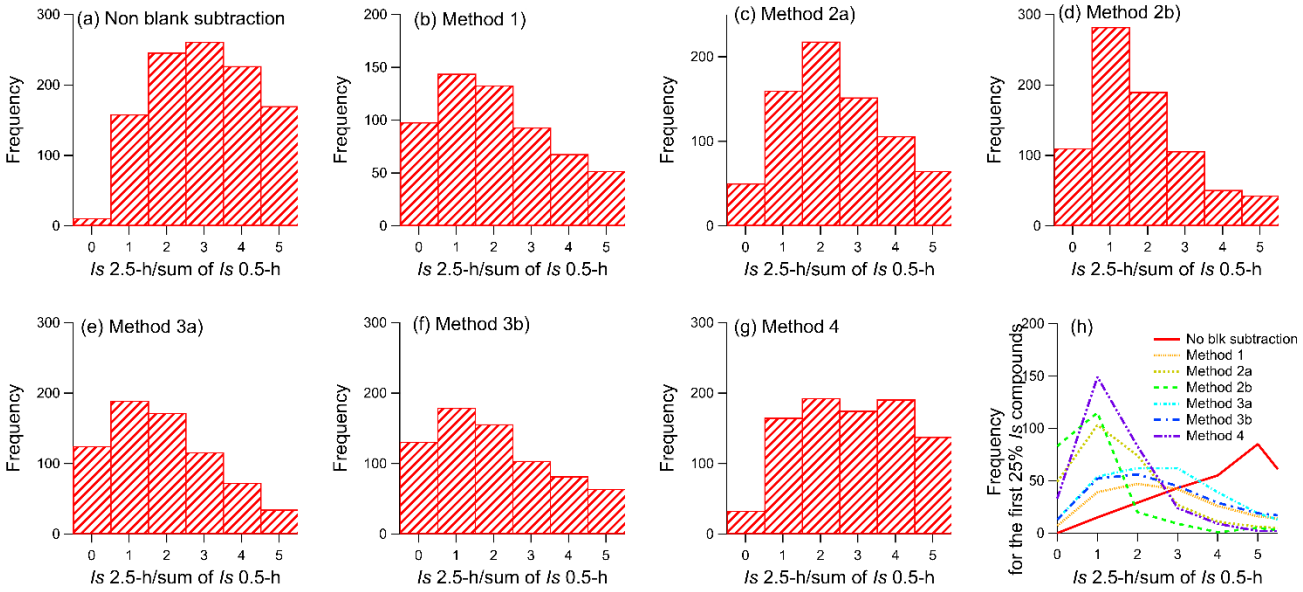

Figure S6. Histogram of the distributions of the *Is* ratios between 2.5-h and the sum of 0.5-h samples with (a) no blank subtraction, (b) Method 1, (c) Method 2a, (d) Method 2b, (e) Method 3a, (f) Method 3b, (g) Method 4, and the distribution of *Is* ratios for the highest 25% signal intensity compounds for all methods based on the 2.5-h sample.

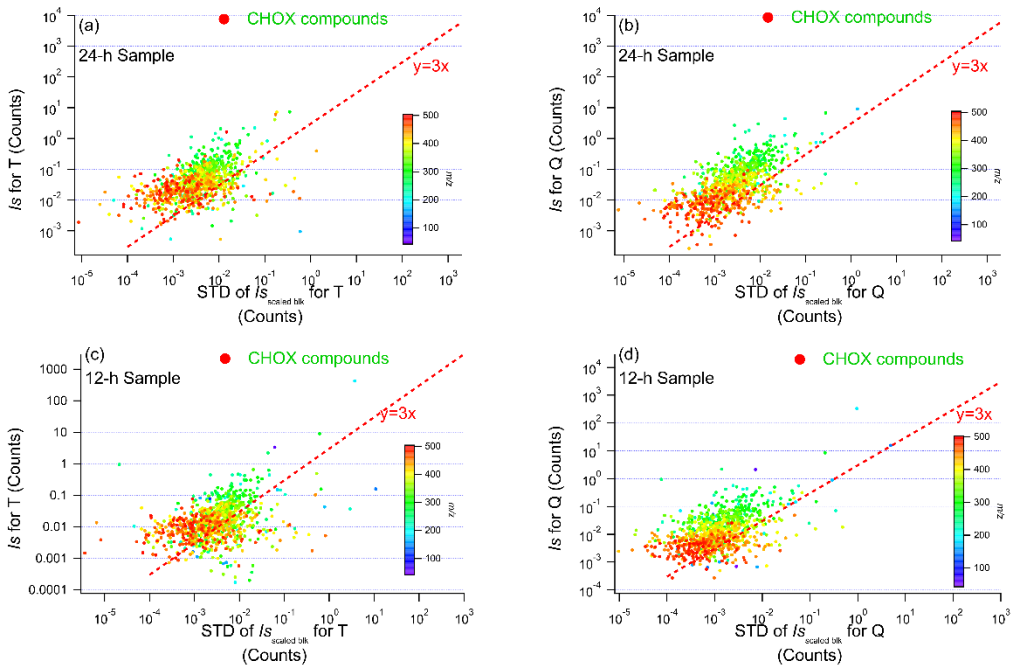

Figure S7. Comparison of the raw CHOX integrated signal intensities (*Is*) and standard deviations of the corresponding backgrounds (scaled field blanks) for (a) 24-h Teflon, (b) 12-h Quartz, (c) 12-h Teflon, and (d) 12-h Quartz samples

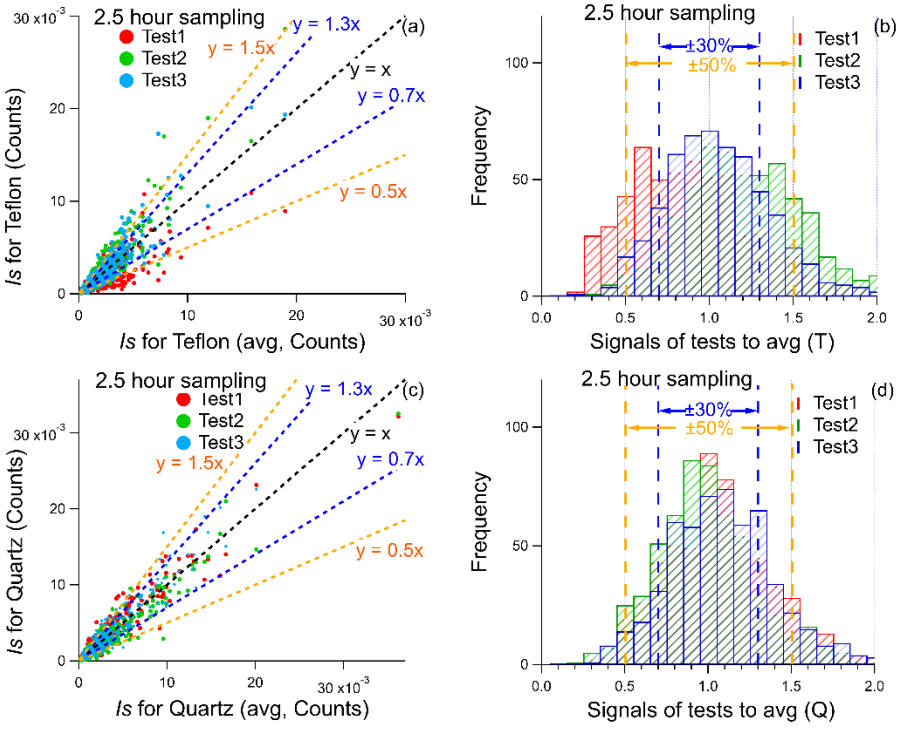

Figure S8. Comparison of the integrated signal intensities for the 3 duplicate tests of the 2.5-h sample for the (a) Teflon and (c) quartz fiber filters, the histogram of the distributions of the ratios of the 3 duplicate tests to their average for (b) Teflon and (d) Quartz fiber filters

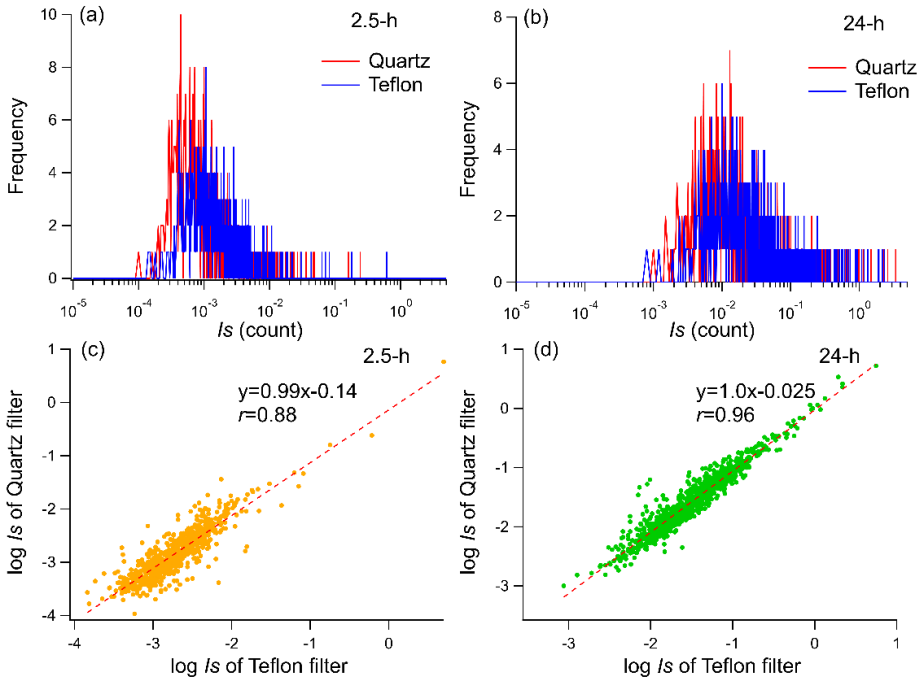

Figure S9. Frequency distribution of the integrated signals of CHOX compounds for Quartz and Teflon samples in (a) 2.5-h collection time (bin width: 1×10^{-5} counts), (b) 24-h collection time (bin width: 1×10^{-4} counts). The correlations between log-transformed *Is* of Quartz and Teflon samples from (c) 2.5-h, and (d) 24-h samples.

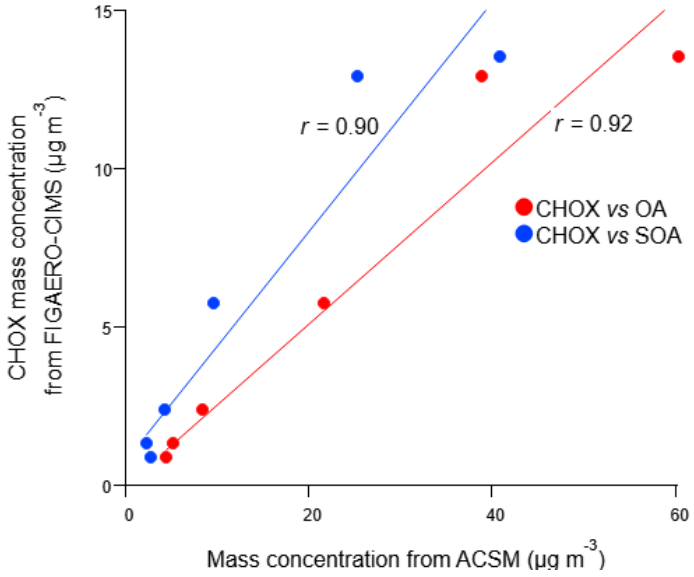

Figure S10. Correlation between CHOX mass concentrations from FIGAERO-CIMS and organic aerosols (OA) as well as secondary organic aerosols (SOA) derived from ToF-ACSM

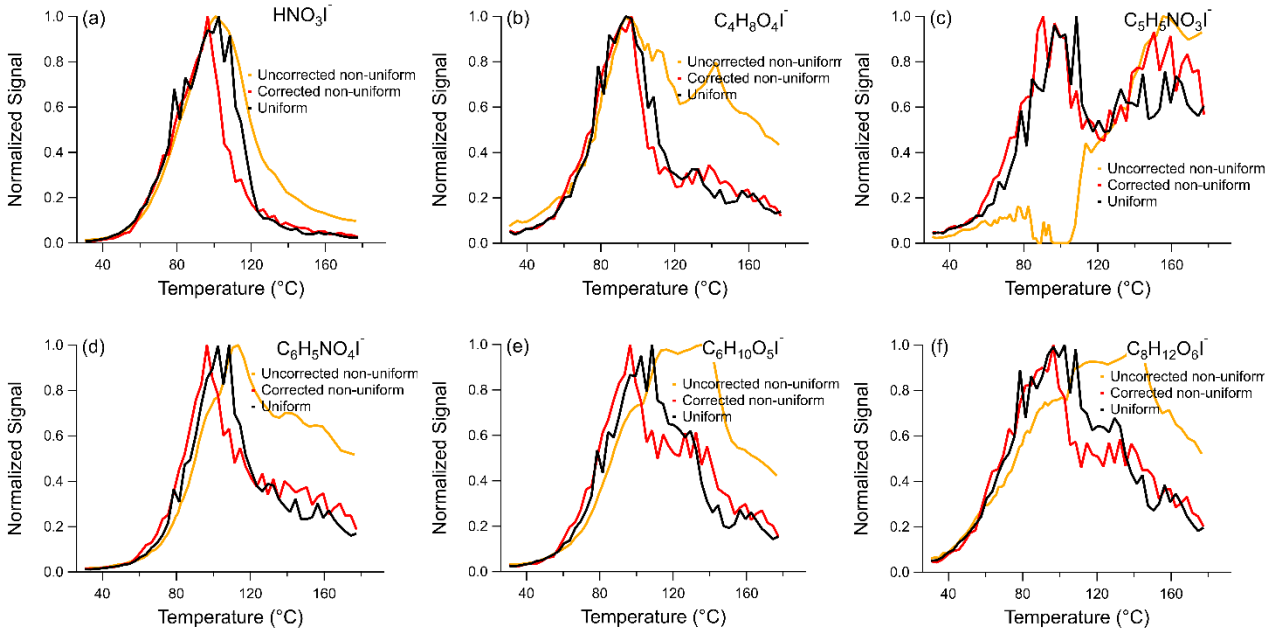

Figure S11. Thermograms (normalized to the highest signal) from the 24h Teflon sample with/without correction from non-uniform ramping and uniform ramping protocols, (a) HNO_3I^-, (b) $C_4H_8O_4I^-$, (c) $C_5H_5NO_3I^-$, (d) $C_6H_5NO_4I^-$, (e) $C_6H_{10}O_5I^-$, (f) $C_8H_{12}O_6I^-$

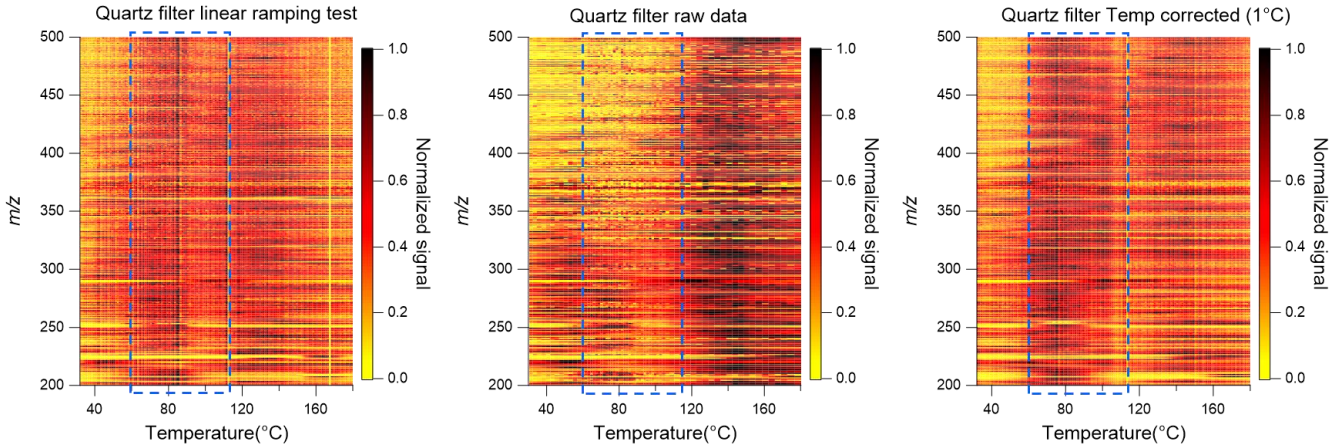

Figure S12. Two-dimensional (2D) thermograms of CHOX compounds for the Quartz filter in (a) the fast linear ramping, (b) the intermediate ramping without correction, and (c) the intermediate ramping after correction. The blue dashed box marks the slow temperature rate region.

Table S1 Sampling information and mass loadings on the punches for the thermogram comparison of different filter types

Sampling date	Sampling time	Filter type	$PM_{2.5}$ loading (μg/2mm punch, 0.031 cm^2)	OA loading (μg/punch)
6-Nov	21:30–9:00	T&Q	0.57	0.38
8-Nov	21:30–9:00	T&Q	1.49	0.61
13-Nov	9:30–21:00	T&Q	4.84	1.01
	21:30–9:00	T&Q	5.57	1.15
24-Nov	9:30–9:00	T&Q (3 duplicate tests)	3.03	1.25